Determination of the surface relaxivity of soft sediment using particle size and shape

Hol, Nick J.; Myouri, Ismail; Chassagne, Claire; Pel, Leo

DOI
10.1016/j.jmro.2025.100198

Publication date
2025

Document Version
Final published version

Published in
Journal of Magnetic Resonance Open

Journal of Magnetic Resonance Open 23 (2025) 100198

Contents lists available at ScienceDirect

Journal of Magnetic Resonance Open

journal homepage: www.sciencedirect.com/journal/journal-of-magnetic-resonance-open

Determination of the surface relaxivity of soft sediment using particle size and shape

Nick J. Hol [a], Ismail Myouri [b], Claire Chassagne [b,*], Leo Pel [a]

[a] Eindhoven University of Technology, Department of Applied Physics, Transport in Permeable Media, P.O. Box 513, 5600 MB Eindhoven, The Netherlands
[b] Delft University of Technology, Faculty of Civil Engineering and Geosciences, Environmental Fluid Mechanics, Box 5048, 2600 GA, Delft, The Netherlands

ARTICLE INFO

Keywords:
NMR
Sedimentation
Consolidation
Surface relaxivity
Kaolinite

ABSTRACT

This study presents a method to determine surface relaxivity in soft sediments by combining one-dimensional Nuclear Magnetic Resonance (NMR) imaging with particle size and shape estimates. In order to determine the surface relaxivity up to now often methods like Mercury Intrusion Porosimetry or Brunauer–Emmett–Teller (BET) are used which where drying steps are involved which can alter material properties during analysis, particularly in highly deformable materials, making these techniques unreliable for soft soils. By combining NMR relaxometry and estimates of particle sizes and shapes of a soft soil, this new approach provides accurate, non-invasive surface relaxivity measurements. This method is demonstrated on kaolinite, glass beads, and natural soils, showing that this method supports detailed assessment of pore size distributions in soft sediments, benefiting geotechnical and environmental research where soil stability is critical.

1. Introduction

Understanding the specific sizes and distributions of pores in natural soils provides critical insights into their material properties. Particularly in materials such as quick clays and sediments found in aquatic environments like lakes, rivers, and oceans, the Pore Size Distribution (PSD) plays a key role in determining essential soil properties, including hydraulic conductivity, permeability, soil sensitivity, and shear strength [7]. These properties are fundamental to geotechnical and environmental research, as they directly influence soil stability, fluid movement, and overall behavior under various loading and environmental conditions.

Determining the PSD of soft materials, particularly those in marine environments, presents challenges. These materials are formed by fine-grained clay particles that settle under gravity, creating water-saturated, soft, consolidated beds over time. Classical methods, such as Mercury Intrusion Porosimetry (MIP) and Brunauer–Emmett–Teller (BET), require the material to be dried beforehand, which can significantly alter the PSD due to the highly deformable nature of soft sediments. Additionally, techniques like Micro Computed Tomography (μCT) often fail to provide pore-level resolution or are prohibitively time-consuming [22].

Nuclear Magnetic Resonance (NMR) offers an alternative, non-destructive approach for determining PSDs in soft sediments. The NMR signal amplitude provides direct information on moisture content and, consequently, on the volume fractions of the sediments, while the rate of signal decay correlates with the material's microstructure and PSD [9,16,21]. Low-field, portable NMR relaxometry systems with spatially small homogeneous magnetic field regions, make this technique cost-effective and broadly applicable, particularly for analyzing PSDs of saturated sediments with fully wetted pores.

However, deriving an accurate PSD from NMR relaxometry requires accounting for surface relaxivity, a material-dependent constant influencing the relaxation signal. Since the NMR relaxation rate is affected by both pore size and surface relaxivity, an independent measurement is typically needed to calibrate the surface relaxivity constant. Various methods have been developed for this calibration, usually combining an independent measurement of the surface-to-volume ratio or Specific Surface Area (SSA) of the pores (e.g., via μCT or MIP) with NMR relaxation data [2]. However, as noted earlier, independent methods often struggle to accurately determine these parameters for soft sediments. Recently, NMR-only methods, such as diffusion-based experiments, have been developed to overcome these challenges, however these methods are still time consuming [8,13].

This study introduces a novel method for determining surface relaxivity in soft sediments using the profile measurement as obtained

* Corresponding author.
E-mail address: C.Chassagne@tudelft.nl (C. Chassagne).

https://doi.org/10.1016/j.jmro.2025.100198

Available online 2 April 2025

by one-dimensional imaging by NMR of the sedimentation proces, combined with independent measurements of particle size and shape, giving access directly to the surface relaxitviy. By using NMR one can capture the sedimentation and consolidation dynamics of marine sediments, including volume fractions and relaxation rates over time and space [10]. By combining this with an an independent estimation of particle shape and size, the pore surface can be inferred and hence enabling the determination of surface relaxivity and thereby the pores-size distribution. Hence this new method offers an efficient and effective way to determine PSDs of soft sediments in situ, during the early phases of consolidation, providing detailed information on the structural properties of these sediments.

In the following section we will first discuss the idea behind the proposed method, followed by its application to a range of materials, including kaolinite clay suspensions, glass beads, and a natural soil, testing this new method.

2. Theory

2.1. Connecting NMR relaxation mechanisms to sedimentation phases of suspensions

Consider a sedimentation column filled with a water-based suspension, as illustrated in Fig. 1. A homogeneous suspension forms a sediment bed as the particles settle under gravity over time, leaving a suspension layer above and a clear water layer at the top. In the primary settling regime, before the so-called gelling point, the system consists of three distinct regions: (1) a suspension layer with homogeneously distributed particles, (2) a loosely packed particle bed, and (3) a particle-free water layer. After the gelling point, in the primary consolidation regime, the entire suspension phase will have sedimented on the particle bed, which consolidates i.e., it will compact in time, leaving a packed particle bed and a clear water layer as a result.

Nuclear Magnetic Resonance (NMR) imaging can be used to study this process. A small-scale 1D NMR scanner with low static fields

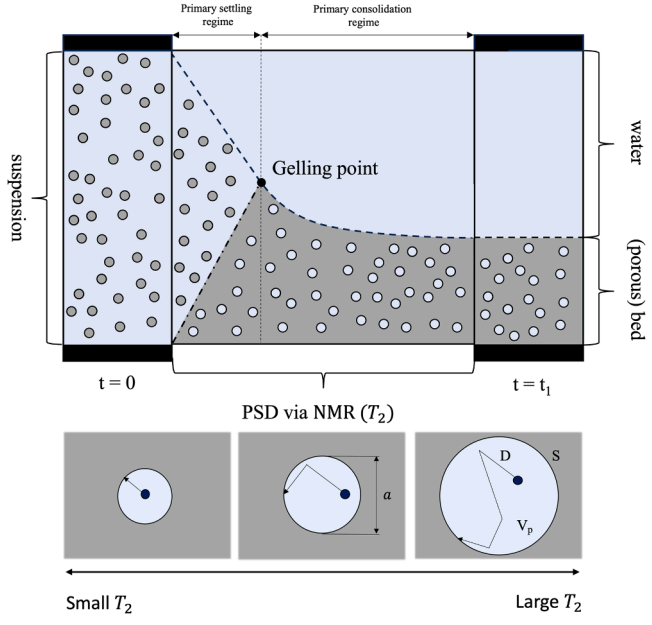

Fig. 1. A schematic representation of a typical sedimentation process from a natural homogenous suspension (left) to a consolidated bed of particles (right). Over time, particles sediment, forming a particle bed. At the gelling point, the suspension phase disappears as all particles have sedimented on the particle bed, forming a soft deformable porous material. The bed itself consolidates over time. The pore size of the bed can be related to the T_2 time of the water in the pores.

(0.78T), static gradients (± 0.1 T/m) and test column of 23 mm diameter and 200 mm length can be used for this purpose. By moving the sedimentation column through the NMR scanner with the help of a stepper motor and by using a multi-slice stepper motor method, sedimentation profiles can be determined with a high spatial and temporal resolution [10]. In this multi-slice stepper motor method, the positions at which slices are measured is interleafed as to make optimal use of the repetition time, which is dominated by the water phase, i.e., TR > $4T_1$~12 s, i.e., a mechanical equivalent of the frequency multi slice method. Hence in this case the CPMG signal decay [6,15] as measured at every slice is dominated by the structural changes in the sedimentation process.

Indeed, within this system the T_2 relaxation depends on two distinct mechanisms depending on whether the measurement is taken in the suspension phase or the particle bed. In the suspension phase, both $1/T_2$ and $1/T_1$ are dependent on the particle concentration. For small colloidal particles that are homogeneously distributed throughout the suspension, the particles act as relaxation centers, effectively increasing the viscosity of the suspension. This leads to a reduction in both T_1 and T_2 of the ^{1}H nuclei in the suspension, see,e.g., [11,20].

In the consolidated particle bed, which is the primary focus of this study, the relaxation behavior gives rise to a different interpretation, i.e., a pore-size distribution. Here, the water molecules interact with the solid surfaces of the sediment particles, which form the pore structure of the bed. T_2 relaxation in this region is predominantly controlled by the surface relaxivity of the sediment particles and the size of the pores in between them. Surface relaxivity itself, in turn, is mainly influenced by the paramagnetic content of the particles and their magnetic susceptibility (see e.g., [18]). As the consolidation progresses and pore sizes decrease, faster relaxation times occur, providing insight into the evolving microstructure of the sediment, as shown in Fig. 1. Here we want to stress that in this case the particle bed forms a soft clayey material which compacts as time progresses, i.e., the pore-size distribution will change during the compaction phase. Hence the pore-size distribution cannot be determined by classical methods like MIP or BET, as these assume a rigid porous medium with a fixed pore size distribution.

In general, relaxation mechanisms contributing to T_2 relaxation can be described as:

$$\frac{1}{T_2} = \frac{1}{T_{2,V}} + \frac{1}{T_{2,S}} + \frac{1}{T_{2,D}} = \frac{1}{T_{2,}V} + \rho_2 \frac{S}{V_p} + \frac{1}{12} D(\gamma\, G\, TE)^2 \quad (1)$$

where $T_{2,V}$, $T_{2,S}$ and $T_{2,D}$ are the bulk, surface, and diffusion relaxation respectively. ρ_2 is the transverse surface relaxivity due to the susceptibility mismatch of the water and the clay surface and TE the echo time. The diffusion-based relaxivity is dependent on the background susceptibility gradient G. As in this research short echo times are used (300 μs), this diffusion-based term is ignored. Furthermore, if one assumes a fast diffusion regime, which is typical for soft clayey sediments with pore sizes on the order of the diffusion length of water molecules, the relationship between pore size and T_2 can be reduced to the following equation [4]:

$$\frac{1}{T_2} = \rho_2 \frac{S}{V_p}. \quad (2)$$

Here ρ_2 is the surface relaxivity, S the pore surface and V_p the pore volume and hence the S/V represents a length scale characterizing the pores size.

2.2. Determining the surface relaxivity by combining NMR relaxation with particle size and shape

Since the pore sizes, and therefore T_2, pore surface area (S), and pore volume (V_P), can vary over the height of the sediment bed, within this study median values are considered in order to estimate the surface relaxivity ρ_2 based on the Brownstein–Tarr model, resulting in:

$$\rho_2 = \frac{1}{\langle T_2 \rangle} \frac{\langle V_p \rangle}{\langle S \rangle} \tag{3}$$

where the values between brackets $\langle \ldots \rangle$ are medians of the parameter within the bracket over height in the particle bed within a single sediment profile.

In order to get an estimate of the pore volume V_p within the sediment bed we can first consider the volume fraction of water as measured by NMR in a slice, which is given by:

$$\phi = \frac{V_p}{V} = \frac{V_p}{V_s + V_p} \tag{4}$$

Here V_p is the pore volume within the excited slice, V_s the solid volume fraction and V the total volume of the selected slice.

The solid volume fraction can now be derived by estimating the total volume of individual particles contained within the slice. In order to do so we make use of the particle shape of the particles contained with the particular suspension. To do so SEM images are taken of the particles as given in Fig. 2. For example, in the case of clay, individual particles can be modeled as platelets, i.e., approximated by cylinders with a height 0.1 times the cylinder's radius r [3]. If we assume that there are n clay platelets in a volume V of a slice, then:

$$V = V_p + V_s = \phi V + n \left(0.1\ \pi\ \langle r \rangle^3\right) \tag{5}$$

The pore surface, S,can also be estimated by using the same particle shape estimation, i.e., a cylindrical approximation for clay particles. The total surface of all kaolinite particles in a slice in this case is given by:

$$S = n\ S_{particle} = n\ \left(2\pi \langle r \rangle^2 + 0.2\pi \langle r \rangle^2\right) \tag{6}$$

By combining Eq (3)-(6), the surface relaxivity in this case of clay particles is given by:

$$\rho_2 = \frac{1}{\langle T_2 \rangle} \frac{\langle r \rangle\ \langle \phi \rangle}{22\ (1 - \langle \phi \rangle)} \tag{7}$$

Hence we can relate the surface relaxivity to the median particle size of particles that make up the porous bed. A similar derivation can be made for the sedimentation of spherical glass beads as also given in Fig. 2. In this case the surface relaxivity is given by:

$$\rho_2 = \frac{1}{\langle T_2 \rangle} \frac{\langle r \rangle \langle \phi \rangle}{3\ (1 - \langle \phi \rangle)} \tag{8}$$

The general form of eq. 7-8 is equivalent, which can be written in its general form as:

$$\rho_2 = \frac{1}{\langle T_2 \rangle} \frac{\langle r \rangle \langle \phi \rangle}{\alpha\ (1 - \langle \phi \rangle)} \tag{9}$$

Here, α now is a geometry factor which is 3 for clay platelets and 22 for spheres. Hence, this method links the median pore structure of a sediment bed to its surface relaxivity, using both NMR relaxation measurements and particle geometry approximations.

The volume fraction of water ϕ and T_2 relaxation in the pores can be extracted from the amplitude of the NMR signal and its relaxation respectively, while for the soft sediments the median particle radius $\langle r \rangle$ (also refered to as D50) can be retrieved from an independent measurement, e.g., by using a diluted suspension and a Laser Diffraction Particle Analyzer. Hence in this proposed method we only have to make an assumption on the individual particle size and shape. No assumption is made of the specific pore geometry, like cylindrical pores in MIP, nor has the sample to be dried. A limitation is that his proposed method assumes one specific particle size, being the D50. Therefore, it is expected that this method will only yields accurate results for particle distributions in suspensions which are narrow.

3. Results

In order to validate the proposed method measurements were performed on five samples using proposed particle shape approximation: three pure kaolinite samples in de-ionized water (KAO_ANG, KAO_IME, KAO_CLA); one natural clay-based sediment dredged from the port of Bremen (NAT_BRE) containing a high amount of (magnetic) impurities; and one sample consisting of glass beads with a well known median particle size (D50) of 120 microns in de-ionized water (GLS). The glass sample is used to provide an analysis of a particle bed which consists particles with a different geometry than clay platelets.

For the pure kaolinite samples, dry kaolinite powders are mixed with de-ionized water and stirred until a homogenous suspension is formed with a kaolinite concentration of 100 g/L. Glass beads are, prior to the measurement, cleaned in a sonic bath for one hour after which 250 g/L

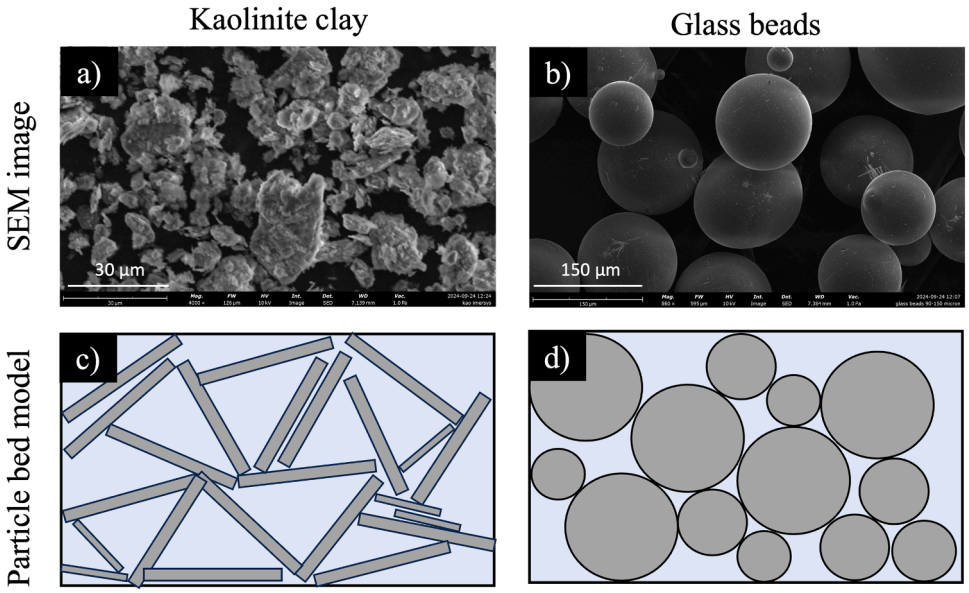

Fig. 2. SEM images of dry kaolinite clay (a) and glass beads (b); Schematic approximations of kaolinite particles as cylindrical platelets in a particle bed (c) and glass beads as spheres in a particle bed (d).

of the glass bead suspension in de-ionized water is created. The Bremen sample (straight out of the harbor) is stirred until a homogenous suspension is created at 280 g/L. Finally, 80 ml of each suspensions is used in 200 mm high, 23 mm wide cylindrical glass tubes and mixed thoroughly before the sedimentation experiment is started.

The samples with homogenous suspension are left to sediment for a minimum of 72 h. In this study a small-scale one-dimensional NMR scanner is used [10]. The NMR setup is schematically represented in Fig. 3. A GMW 3473-70 Electromagnet is used to generate a static magnetic field (B_0) of 0.78 T. A Faraday shield is used to shield the high-frequency coils of the NMR system, making the NMR measurements quantitative [12,17]. Changes in the dielectric properties of the volume contained within the coil as the samples moves through the NMR will change the tuning of the LC circuit. Implementing a Faraday shield consisting of vertical wires only will allow the magnetic field lines to pass through the shield, while shielding the electric field lines, preventing detuning of the LC circuitry.

As indicated, in order to measure a profile a multi-slice stepper motor method is used as to decrease the measurement time of a profile as this dominated by the repetition time of the water phase, i.e., $TR > 4T_1 \sim 12$ sec. In this multi-slice stepper motor method care is taken that the maximum acceleration of the stepper motor does not exceed 1% of the gravitational acceleration. At every slice, a Carr–Purcell–Meiboom–Gill (CPMG) sequence with 2048 pulses and an echo time (TE) of 300 μs was used at a constant magnetic gradient of 0.11 T/m. With a pulse duration of 30 μs, a slice of approximately 3 mm thick is excited. The signal intensity in the slice can be directly related to pore volume V_p and water volume fraction ϕ, while signal decay is used to derive T_2.

In Fig. 4. we have given both the volume fractions of water ϕ and T_2 time as a function of the height of all 5 samples at the end of consolidation, i.e., after 72 h. As can be seen from the figure, the natural

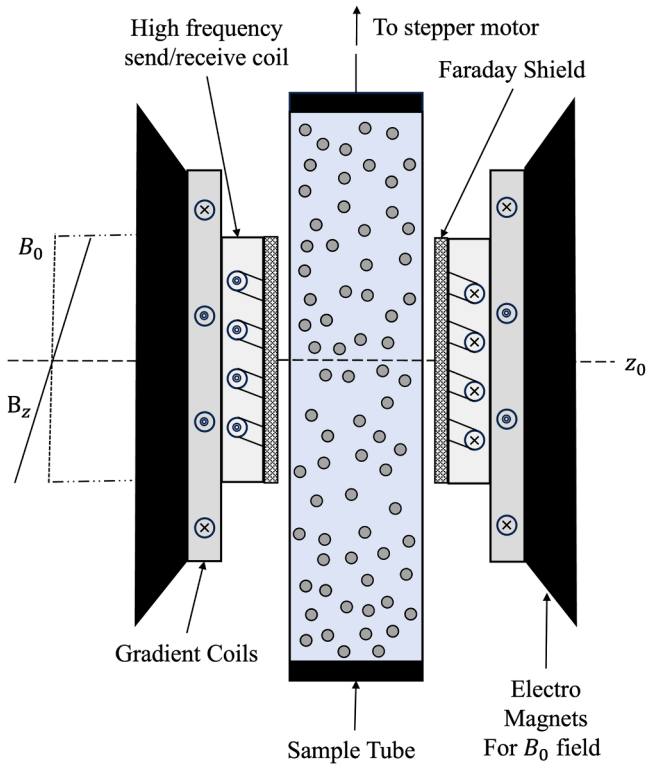

Fig. 3. Schematic representation of the NMR setup. The electromagnet produces a static magnetic field (B_0) of 0.78T. Gradient coils produce a constant magnetic gradient of 0.11 T/m along the height of the sample. The high frequency RF coil is shielded from the sample by a Faraday shield. The sedimentation columns (sample tube) can be moved through the NMR with a stepper motor connected with the sample.

Bremen sediment has the lowest T_2 distribution, which can be attributed to the large amount of impurities in this natural sample. Glass has the highest T_2 on average. Except for the glass samples, all T_2 distributions show an upward curve over the height of the sample as expected, indicating that pores become larger as we move up the height of the sediment column.

The median values of T_2 time $\langle T_2 \rangle$ and volume fraction $\langle \phi \rangle$ from Fig. 4 are given in Table 1. As can be seen the glass sample exhibits the lowest median volume fraction at 0.37, closely aligning with the expected volume fraction of 0.365 for randomly packed homogeneous spheres [23]. The pure kaolinite samples exhibit similar median T_2 times due the natural sediment having the lowest median T_2 value due to the larger amount of impurities.

Next, the D50 of the kaolinite and natural sediments is estimated using a Malvern Mastersizer 3000+ Laser Diffraction Particle Analyzer. In order to do so the clay-based sediment suspensions are diluted to contain <1 g/L sediment. The diluted suspensions are fed through the analyzer, yielding particle size distribution as given in Fig. 5.

As can be seen from Fig. 5, the kaolinite-based suspensions have a narrow particle-size distribution with peaks around 10 micron. The natural Bremen sediment (NAT_BRE) has a broader particle distribution, skewed towards larger particle sizes, with a peak around 10 micron as well. Based on the measured particle size distributions (given in Fig. 5), the D50 is calculated for each clay sample and these are given in Table 2. As can be seen the D50 is dominated by the smallest particles from the sediment suspensions.

Based on the determined $\langle T_2 \rangle$, $\langle \rho_2 \rangle$, $\langle \phi \rangle$ from Table 1 and D50 from Table 2 we can now determine the surface relaxivity at the end of the consolidation. These results are given in Table 2. For clay-based samples, eq. (7) is used while eq. (8) applies for the glass beads. As can seen all pure kaolinite samples yield a surface relaxivity between 21.5–25.3 μm/s, whereas the natural bremen sediment (NAT_BRE) and glass beads (GLS) have a surface relaxivity of 291.8 μm/s and 48.6 μm/s respectively.

In order to relate the determined surface relaxivity to their iron content we have performed X-Ray Fluorescence (XRF) measurements on dried samples. The results are also given Table 2. As can be seen for the clay-based sediments, the surface relaxivity correlates well with the iron content. Indeed, the surface relaxivities for the kaolinite samples are in good agreement with similar research by Elsayed et. Al, which showed that kaolinite samples with 1 wt% iron content should have a surface relaxivity of around 28.2 μm/s [9].The surface relaxivity of the natural Bremen sediment (NAT_BRE) of 291.8 μm/s again correlates with the high iron content caused by the natural impurities in the soil. Similar surface relaxivities of 360 ± 50 μm/s are reported for natural soils via NMR Diffusion experiments by [8]. The surface relaxivity of 48.6 μm/s for the glass beads sample (GLS) is slightly above the range of surface relaxivities found for similar silica-based glass samples ranging from 22.6–45 μm/s determined via μCT [1,9].

It is to be noted that while most examined samples are well characterized by the fast-diffusion limit (with Brownstein-Tarr number $\frac{\rho * 2D50}{D} \ll 1$), the NAT_BRE samples is in the intermediate diffusion regime (with Brownstein-Tarr number $\frac{\rho * 2D50}{D} > 1$). The intermediate regime is characterized by more complex relaxation dynamics, with higher relaxation modes becoming noticeable. As these are not taken into account in this method, the retrieved surface relaxivity in the case of the NAT_BRE sample should be seen as a first-order estimate.

4. Discussion

We have also determined the surface relaxivity of the clay-based samples using standardized BET measurements [5]. In order to do so clay sediments are dried in an oven at 60 °C until constant mass. A coarse powder is made by scraping the dried sediment with a spoon, and weighted. The sample is additionally dried for a further 24 h under

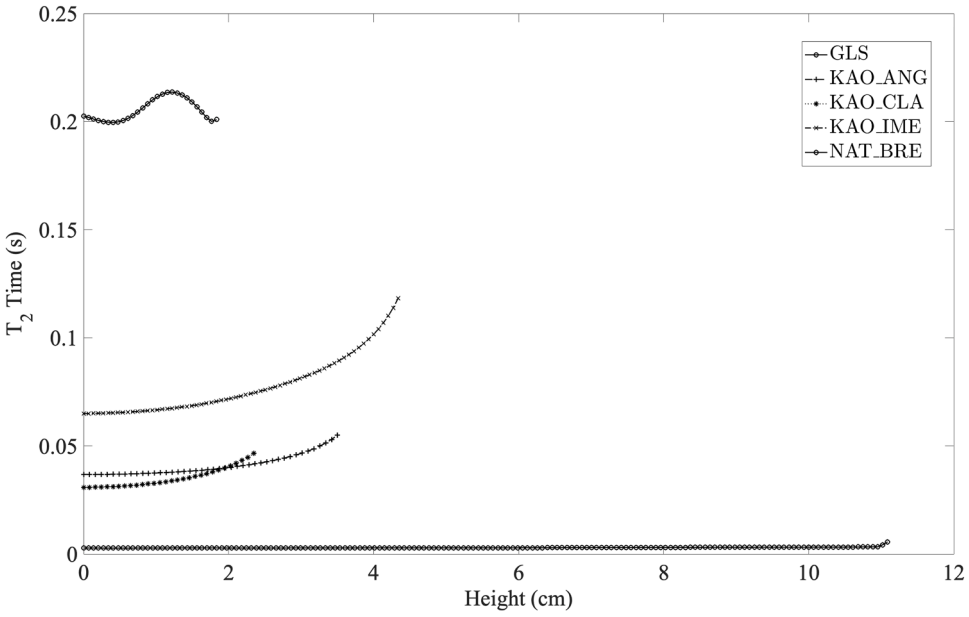

a) T_2 time of water in porous particle bed of various samples

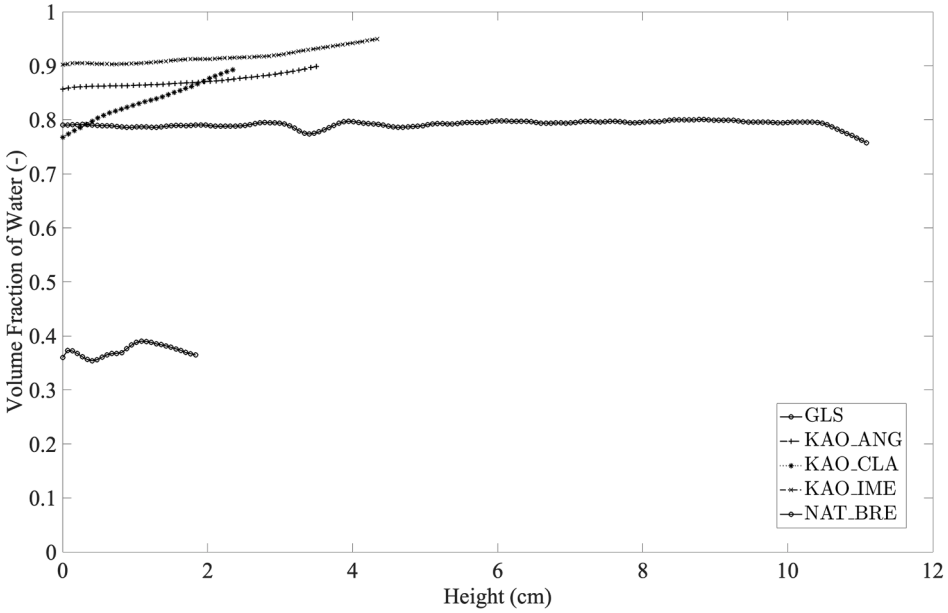

b) Volume fractions of water in porous particle bed of various samples

Fig. 4. a) T_2 times of water in porous particle bed of various clay and glass-based samples; b) volume fractions ϕ of water in the porous bed of clay and glass-based samples; The median values of T_2 and ϕ are indicated within the graphs.

Table 1
Calculated median T_2 time $\langle T_2 \rangle$ and volume fraction $\langle \phi \rangle$ in the consolidated particle bed for clay-based and glass beads samples, after 72 h.

Sample [-]	$\langle T_2 \rangle$ (s)	$\langle \phi \rangle$ $(-)$
GLS	0.20	0.37
KAO_ANG	0.04	0.87
KAO_CLA	0.04	0.83
KAO_IME	0.08	0.92
NAT_BRE	0.003	0.79

nitrogen flow in a micrometrics FlowPrep 060 at 160 °C. Finally the specific Surface Area (SSA) is determined using a micrometrics Gemini VII Surface Area and Porosity Analyzer (BET).

The SSA is used to derive the surface relaxivity combined with the NMR experiments (where the mass of the sample is calculated from the volume and density of the suspension, and T_2 time from Table 1 is used). Both specific surface area (SSA) and surface relaxivity derived via BET are given in Table 2.

As can be seen the surface relaxivity values via BET consistently yield smaller values by a factor of 5–8 than via the proposed method of particle size and shape approximation. A similar low ρ_2 values of 1.8 on kaolinite was also reported by Matterson *et. al.* which also used BET

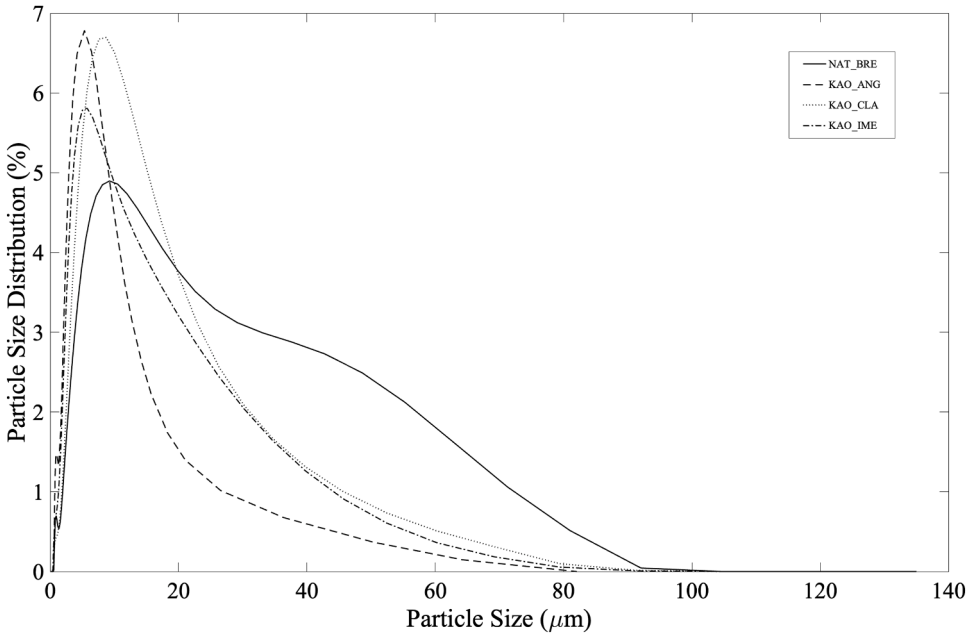

Fig. 5. Particle size distributions of clay-based sediments, both natural sediment (NAT_BRE) and pure kaolinite samples (KAO_CLA, KAO_IME and KAO_ANG) as determined by Laser Diffraction Particle Analysis with sediment suspensions diluted to < 1 g/L.

Table 2
Calculated surface relaxivities for clay-based and glass beads samples via particle size/shape and BET methods. Surface relaxivities are related to their iron content, median particle size (D50) and specific surface area (SSA).

Sample [-]	D50 [μm]	ρ_2 [μm/s] via particle shape and size	SSA_{BET} [cm^2/g]	ρ_2 [μm/s] via BET	Iron content Fe_2O_3 [%]
NAT_BRE	10.1	291.8	19.1	43.0	12.5
KAO_CLA	7.8	25.3	16.3	3.2	1.59
KAO_ANG	6.4	24.2	12.6	5.0	1.45
KAO_IME	6.6	21.5	14.2	3.2	1.12
GLS	120	48.6	n.a.	n.a.	0.36

[14]. This can be explained by looking more closely at the length scales and surface morphologies at which these two methods (BET and NMR) are sensitive. Within the NMR measurements, the surface is probed by water molecules which diffuse through the macropores created between the stacked clay particles. The dephasing length is on the order of microns, i.e., on the order of the macropores one measures via NMR. Trapped water molecules in nanopores within the particles of the particle bed do not contribute to the NMR signal due to fast relaxation [19]. This is of no interest in these experiments as our focus lies on the larger pores in between particles in the sedimentation column, where water diffusion is probing the pore space. BET, however, measures adsorption of gases using gas isotherms. The surface averaging therefore takes place on the length scale of the gas molecule (order of nanometers). Therefore, BET measures both the surface area of nanoporous and macro structure of the material, and hence overestimates the surface of the macro pores which is needed to get a correct estimate for the water molecules diffusion only within the macro pores. Indeed [8], found similar differences for the surface relaxivity in the order of 2–6 between BET and NMR (diffusion).

It is important to note that the proposed surface relaxivity determination method may only be used if particle beds of sediments are consolidated. To see this effect, we investigate how the determined surface relaxivity evolves over time as the particle bed is formed and consolidates. To this end, a typical sedimentation process from a homogenous suspension to a consolidation of two pure kaolinite samples (KAO_ANG and KAO_CLA) is investigated. The sedimentation process is studied for the first 36 h of consolidation. An entire sedimentation profile is measured every 15 min with the 1D NMR protocol [10].

The complete sedimentation process is given in Fig. 6, where both the volume fractions of water as the PSD over the height of the particle bed (via Eq. (2)) is given. As explained in Fig. 1, the initially homogenous suspension settles under the influence of gravity. For both samples, the particle bed increases at first until the gelling point is reached. As all particles have sedimented on the bed, the bed then consolidates until a quasi-steady system is created.

Consolidation and sedimentation show differences over time depending on the sample. This can be attributed to the difference in pH value of the suspensions, which is 4.9 for KAO_ANG and 8.3 for KAO_CLA. More specifically, this difference in pH influences the surface charge of kaolonite particles in the suspension. For KAO_CLA, in basic conditions, face-to-face stacking of the kaolinite platelets occurs. For KAO_ANG on the other hand, where platelets are in an acidic environment, platelet stacking prefers a more edge-to-face configuration upon sedimentation and consolidation. This edge-to-face configuration (KAO_ANG) provides a more rigid and less compact homogenous structure, similar to a house of cards, than the face-to-face stacking which provides a less rigid and more compact structure (KAO_CLA) [7].

Based on these measurements, we can now determine the surface relaxivity at each time step, with the results presented in Fig. 7. For both kaolinite samples, KAO_ANG and KAO_CLA, the surface relaxivity asymptotically levels off to a constant value as the particle bed consolidates. This behavior can be explained by the relationship between the particle size distribution of the suspension and the formation of the particle bed. Specifically, the determination of surface relaxivity is only valid after the gelling point is reached and all particles have settled onto the consolidating particle bed. After the gelling point, the D50 value, derived from the suspension, accurately represents the D50 of the particles within the bed. Moreover, as the consolidation progresses, the pores in the bed become more distinct, allowing the relaxation behavior to be better described by the Brownstein-Tarr theory, which links pore size, T_2 relaxation times, and surface relaxivity.

In Fig. 7, it can be seen that the surface relaxivity of KAO_ANG levels off much more quickly (around 6–7 h) than for KAO_CLA (around 25 h). This difference can be attributed to the different pH environments of the samples. As highlighted before, the edge-to-face configuration of

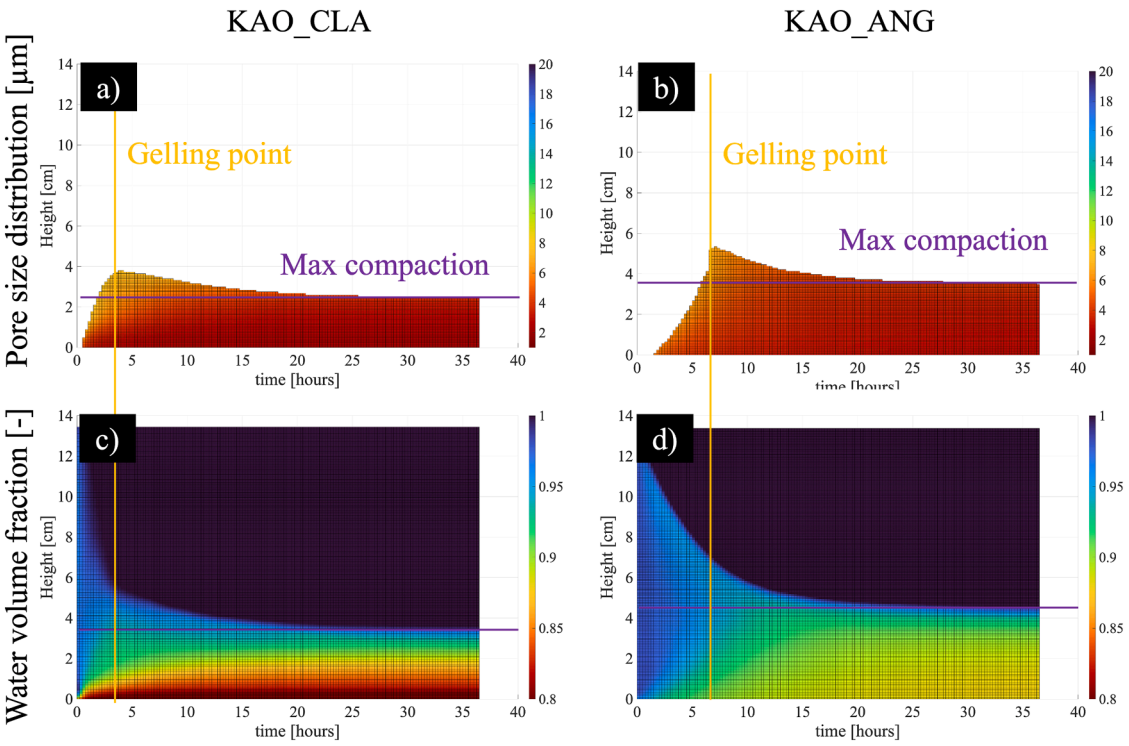

Fig. 6. Pore Size distributions over the height of the sample in the particle bed and volume fraction of water in the sedimenting kaolinite clay profiles in deionized water over time. The columns start of as a homogenous suspension. Over time, a particle bed is formed and a clear water layer forms.

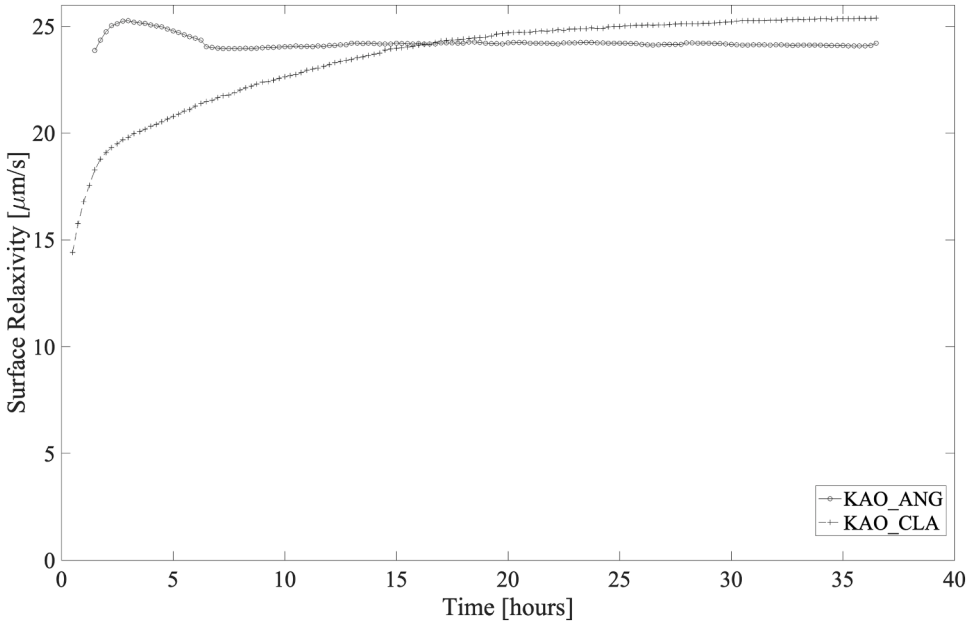

Fig. 7. The surface relaxivities of sedimenting kaolinite mixtures determined as a function of time for KAO_ANG and KAO_CLA via Eq. (6).

KAO_ANG platelets provide a rigid and less compact homogenous cardhouse structure, which becomes stable soon after the gelling point has been reached. For KAO_CLA on the other hand, the face-to-face stacking which provides a less rigid and more compact structure (KAO_CLA) which takes more time to consolidate and become stable.

5. Conclusion

The proposed new method for determining surface relaxivity using NMR imaging and particle size and shape approximations provides a means to assess surface relaxivity in soft sediments, where traditional techniques like MIP or BET analysis are limited in their application. Validation experiments and comparisons with established research demonstrate the method's applicability to a variety of of clay-based samples and glass spheres. Results are in agreement with previous findings on similar samples and show a correlation between NMR-derived surface relaxivities and sediment characteristics, such as iron (Fe_2O_3) content.

It should be noted that the proposed method for determining surface relaxivity is accurate only when the particle bed has fully consolidated. Additionally, the method has been tested on samples with narrow particle size distributions, typically in the range of tens of microns. A limitation of the approach is its reliance on the median particle size (D50), to approximate surface relaxivity, which may limit its applicability for samples with broader particle size distributions.

Future research could address this limitation by integrating over the full particle size distribution rather than relying solely on median particle size. This adaptation would potentially increase the method's robustness and applicability to samples with broader PSDs, allowing for a more comprehensive assessment of surface relaxivity across diverse sediment types.

Ethics declarations

Not applicable.

Declaration of generative AI and AI-assisted technologies in the writing process

During the preparation of this work the authors used ChatGPT in order to check for spelling, grammar and improve sentence structuring. After using this tool/service, the authors reviewed and edited the content as needed and take full responsibility for the content of the published article.

Funding

This project has been made possible partly due to the the Sediment to Soil project (S2S) : NWO Open technology program grant 2020-II TTW ref. 13314.

CRediT authorship contribution statement

Nick J. Hol: Writing – review & editing, Writing – original draft, Visualization, Validation, Software, Investigation, Formal analysis, Data curation, Conceptualization. **Ismail Myouri:** Writing – review & editing, Investigation, Data curation. **Claire Chassagne:** Writing – review & editing, Supervision, Funding acquisition, Data curation, Conceptualization. **Leo Pel:** Writing – review & editing, Validation, Supervision, Resources, Conceptualization.

Declaration of competing interest

The authors declare that they have no known competing financial interests or personal relationships that could have appeared to influence the work reported in this paper.

Acknowledgements

The authors would like to acknowledge Joey Aarts (TU Eindhoven, Netherlands) for his help on the BET measurements. The authors would also like to thanks the TU Delft MUDNET community for the overall support and sparring sessions during the project.

Supplementary materials

Supplementary material associated with this article can be found, in the online version, at doi:10.1016/j.jmro.2025.100198.

Data availability

Data will be made available on request.

References

[1] F. Benavides, R. Leiderman, A. Souza, G. Carneiro, R. Bagueira de Vasconcellos Azeredo, Pore size distribution from NMR and image based methods: a comparative study, J. Pet. Sci. Eng. 184 (2020) 106321, https://doi.org/10.1016/j.petrol.2019.106321.
[2] F. Benavides, R. Leiderman, A. Souza, G. Carneiro, R. Bagueira, Estimating the surface relaxivity as a function of pore size from NMR T2 distributions and micro-tomographic images, Comput. Geosci. 106 (2017) 200–208, https://doi.org/10.1016/J.CAGEO.2017.06.016.
[3] F. Bergaya, G. Lagaly, Handbook of Clay Science, 5, Elsevier, 2013, https://doi.org/10.1016/B978-0-08-098258-8.00001-8.
[4] K.R. Brownstein, C.E. Tarr, Importance of classical diffusion in NMR studies of water in biological cells, Phys. Rev. A 19 (6) (1979) 2446, https://doi.org/10.1103/PhysRevA.19.2446.
[5] S. Brunauer, P.H. Emmett, E. Teller, Adsorption of gases in multimolecular layers, J. Am. Chem. Soc. 60 (2) (1938) 309–319, https://doi.org/10.1021/ja01269a023.
[6] H.Y. Carr, E.M. Purcell, Effects of diffusion on free precession in nuclear magnetic resonance experiments, Phys. Rev. 94 (3) (1954) 630, https://doi.org/10.1103/PhysRev.94.630.
[7] C. Chassagne, Introduction to Colloid Science: Applications to Sediment Characterization, TU Delft OPEN Books, 2021, https://doi.org/10.34641/MG.16.
[8] M. Duschl, P. Galvosas, T.I. Brox, A. Pohlmeier, H. Vereecken, In situ determination of surface relaxivities for unconsolidated sediments, Water Resour. Res. 51 (8) (2015) 6549–6563, https://doi.org/10.1002/2014WR016574.
[9] M. Elsayed, A. El-Husseiny, S.R. Hussaini, M. Mahmoud, Experimental and simulation study on the estimation of surface relaxivity of clay minerals, Geoenergy Sci. Eng. 230 (2023) 212260, https://doi.org/10.1016/J.GEOEN.2023.212260.
[10] N.J. Hol, L. Pel, M. Kurvers, et al., Fast 1D NMR imaging of clay sedimentation using a multi-slice stepper motor method, Exp. Fluids 66 (2025) 9, https://doi.org/10.1007/s00348-024-03937-3.
[11] E.K. Jang, I. Yu, 1H NMR of water influenced by suspended magnetic particles, Colloids Surf. A: Physicochem. Eng. Asp. 72 (C) (1993) 229–236, https://doi.org/10.1016/0927-7757(93)80471-P.
[12] K. Kopinga, L. Pel, One-dimensional scanning of moisture in porous materials with NMR, Rev. Sci. Instrum. 65 (12) (1994) 3673–3681, https://doi.org/10.1063/1.1144491.
[13] Luo, Z.-X., Paulsen, J., & Song, Y.-Q. (2015). *Robust determination of surface relaxivity from nuclear magnetic resonance DT 2 measurements*. https://doi.org/10.1016/j.jmr.2015.08.002.
[14] A. Matteson, J.P. Tomanic, M.M. Herron, D.F. Allen, W.E. Kenyon, NMR relaxation of clay/brine mixtures, SPE Reserv. Eval. Eng. 3 (05) (2000) 408–413, https://doi.org/10.2118/66185-PA.
[15] S. Meiboom, D. Gill, Modified spin-echo method for measuring nuclear relaxation times, Rev. Sci. Instrum. 29 (8) (1958) 688–691, https://doi.org/10.1063/1.1716296.
[16] M. Müller-Petke, R. Dlugosch, J. Lehmann-Horn, M. Ronczka, Nuclear magnetic resonance average pore-size estimations outside the fast-diffusion regime, Geophysics 80 (3) (2015) D195–D206, https://doi.org/10.1190/GEO2014-0167.1.
[17] L. Pel, P.A.J. Donkers, K. Kopinga, J.J. Noijen, 1H, 23Na and 35Cl imaging in cementitious materials with NMR, Appl. Magn. Reson. 47 (3) (2016) 265–276, https://doi.org/10.1007/s00723-015-0752-6.
[18] Saidian, M., & Prasad, M. (2015). *Effect of mineralogy on nuclear magnetic resonance surface relaxivity: a case study of Middle Bakken and three forks formations*. https://doi.org/10.1016/j.fuel.2015.08.014.
[19] F. Stallmach, C. Vogt, J. Kärger, K. Helbig, F. Jacobs, Fractal geometry of surface areas of sand grains probed by pulsed field gradient NMR, Phys. Rev. Lett. 88 (10) (2002) 105505, https://doi.org/10.1103/PhysRevLett.88.105505.
[20] C. Totland, R.T. Lewis, W. Nerdal, 1H NMR relaxation of water: a probe for surfactant adsorption on kaolin, J. Colloid Interface Sci. 363 (1) (2011) 362–370, https://doi.org/10.1016/J.JCIS.2011.07.064.
[21] R.M.E. Valckenborg, L. Pel, K. Hazrati, K. Kopinga, J. Marchand, Pore water distribution in mortar during drying as determined by NMR, Mater. Struct. 34 (10) (2001) 599–604, https://doi.org/10.1007/BF02482126.
[22] L. Vásárhelyi, Z. Kónya, Á. Kukovecz, R. Vajtai, Microcomputed tomography–based characterization of advanced materials: a review, Mater. Today Adv. 8 (2020) 100084, https://doi.org/10.1016/j.mtadv.2020.100084.
[23] Y. Wu, Bulk and interior packing densities of random close packing of hard spheres, J. Mater. Sci. 38 (9) (2003) 2019–2025, https://doi.org/10.1023/A:1023597707363.